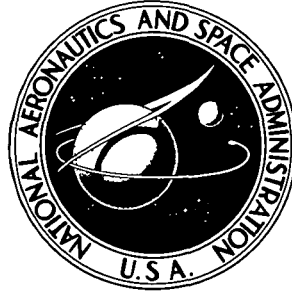


NASA TECHNICAL NOTE



NASA TN D-8505

NASA TN D-8505

**SPECTRAL ANALYSIS
OF A HIGH-VELOCITY METEOR**

Gale A. Harvey

Langley Research Center

Hampton, Va. 23665

1 Report No NASA TN D-8505	2 Government Accession No	3 Recipient's Catalog No	
4 Title and Subtitle SPECTRAL ANALYSIS OF A HIGH-VELOCITY METEOR		5 Report Date July 1977	6 Performing Organization Code
		8 Performing Organization Report No L-11433	10 Work Unit No 506-16-36-02
7 Author(s) Gale A. Harvey	9 Performing Organization Name and Address NASA Langley Research Center Hampton, VA 23665		11 Contract or Grant No
12 Sponsoring Agency Name and Address National Aeronautics and Space Administration Washington, DC 20546			13 Type of Report and Period Covered Technical Note
15 Supplementary Notes			
16 Abstract A spectrogram of a fast optical meteor was reduced and analyzed, and 60 features were identified in the spectrum. Air and ionized elements in this meteor radiate throughout the spectrum from 3000 Å to 6800 Å. A mass of 9 mg and an effective radiation temperature of approximately 5700 K were computed for the meteor. Weight ratios of Ca Fe, Mg.Fe, and Na.Fe were computed. A plasma particle velocity distribution for meteors was derived, and the average collision speed obtained from this distribution was compared with the relative collision speed of a Fe-N ₂ gas mixture at 5700 K.			
17 Key Words (Suggested by Author(s)) Meteor spectra Radiation temperature Meteor composition		18 Distribution Statement Unclassified - Unlimited Subject Category 88	
19 Security Classif (of this report) Unclassified	20 Security Classif (of this page) Unclassified	21 No of Pages 21	22 Price* \$3.50

SPECTRAL ANALYSIS OF A HIGH-VELOCITY METEOR

Gale A. Harvey
Langley Research Center

SUMMARY

A spectrogram of a fast optical meteor was reduced and analyzed, and 60 features were identified in the spectrum. Air and ionized elements in this meteor radiate throughout the spectrum from 3000 Å to 6800 Å. A mass of 9 mg and an effective radiation temperature of approximately 5700 K were computed for the meteor. Weight ratios of Ca:Fe, Mg:Fe, and Na:Fe were computed. A plasma particle velocity distribution for meteors was derived, and the average collision speed obtained from this distribution was compared with the relative collision speed of a Fe-N₂ gas mixture at 5700 K.

INTRODUCTION

The NASA Langley Research Center (LaRC) has been active in meteor physics research since 1963. The research program began as a cooperative effort with the Smithsonian Astrophysical Observatory (SAO) and consisted of a series of rocket flights to simulate natural meteor conditions (ref. 1). The primary task of the research effort was to reduce the uncertainty in determining masses of optical meteors through better measurements of the meteor "luminous efficiency" parameter. This research effort succeeded in reducing the uncertainty in determining masses of optical meteors from 2 orders of magnitude to approximately a factor of 3.

These initial studies in meteor research were not concerned with meteoroid composition. To investigate meteoroid composition, the meteor spectral research program evolved from the NASA-SAO luminous efficiency program and used spectroscopy to study composition of meteoroids in the mass range from 0.001 g to 1 g. Most of the meteor spectra were obtained from meteor patrols in southern New Mexico.

The NASA LaRC Faint Meteor Spectra Patrol (ref. 2) began yielding optical meteor spectra on a continuous basis in November 1968, and over 250 meteor spectra were obtained from the patrol in calendar year 1969. The patrol obtained spectra of faint (+4 to -3 magnitude) optical meteors over the extended spectral range from 3000 Å to 7000 Å and had provisions for absolute calibration. The patrol used in-house designed and fabricated, low f-number, Maksutov slitless spectrographs and photoelectric meteor-detection shutter systems. The sensitivity of the spectrograph systems is roughly 10 times that of previous generation meteor spectrographs. This means that most of the spectra obtained by the patrol are from the free molecular flow regime and not from the slip, transition, or continuum flow regimes characteristic of spectra of similar quality obtained by earlier investigators. It should be noted that

little quantitative spectral analysis, other than that of two very bright meteors (refs. 3 and 4), had been attempted before the NASA program.

The purpose of this paper is to report the data reduction of the first high-definition meteor spectrum from the NASA LaRC Faint Meteor Spectra Patrol. The paper then introduces a technique for the analysis of the radiative processes of faint optical meteors and applies it to the meteor spectrum.

SYMBOLS

A	Einstein probability coefficient of atomic state, sec^{-1}
B(T)	partition function of element
C, C'	constants
E	energy of atomic state above ground state, eV
g	statistical weight of atomic state
h	Planck's constant
I	line intensity
k	Boltzmann constant
m	atomic mass
N	number of atoms
N(V)	speed distribution
T	temperature, K
T_{ij}^*	meteor temperature parameter, K
t	time
V	particle speed, km/sec
V_r	relative collision speed, km/sec
V_{rms}	root-mean-square speed, km/sec
V_0	initial speed of meteoric particle, km/sec
V_1	lowest characteristic speed of particles for excitation, km/sec
λ	wavelength, \AA
λ_{max}	maximum wavelength, \AA

λ_{tab} wavelength of multiplet or line taken from literature
(see table I), Å

ν frequency of radiation

Subscripts:

a,b designates elements (e.g., FeI)

B Boltzmann speed distribution

i,j ith, jth atomic states

m meteoric particles

A bar over a symbol denotes average.

DATA

A high-velocity meteor was photographed in the early morning of November 21, 1968, over southern New Mexico. The meteor was photographed with an f/0.83, 150-mm-aperture Maksutov-type slitless spectrograph. The spectrograph has an inverse dispersion of 500 Å/mm which is intermediate in resolution between the high-resolution and low-resolution spectrographs of the NASA LaRC Faint Meteor Spectra Patrol (ref. 2). The meteor is intermediate in brightness between the fainter and brighter meteors photographed by the patrol and, in this sense, may be considered representative of the patrol spectra. The projected trail of the meteor passed near the Leonid radiant. The relative intensities from the auroral green line of OI and from OI, NI, N₂, CaII, MgII, SiII, and FeII confirm a velocity of 60 km/sec, or higher.

This spectrum is quite similar to Russell's 1958 spectrum of the upper trail of a -2 magnitude Perseid obtained with a 46-cm (18-in.) Schmidt telescope with an objective prism (ref. 5). The relative strengths of multiplets 4, 5, 20, 21, 23, and 24 of FeI; of multiplet 3 of MgI; and of lines of CaII, MgII, and SiII are in general accord in the two spectra. The NASA spectrum is also in general accord with the lower definition faint fast spectra of Millman, Cook, and Hemenway (ref. 6) and Russell (ref. 7).

The spectrum, reproduced from reference 2, is shown in figure 1. The spectrum differs from previously published high-velocity spectra (refs. 8 to 10) of similar quality in three respects: the weakness of the H- and K-lines of CaII, the strength and number of lines whose wavelengths are less than 3900 Å, and the amount of air radiation in the spectrum. The H- and K-brightness behavior probably results from low-energy electron excitation and not from resonant charge exchange with N₂⁺, as discussed by Hoffman (ref. 11), Harvey (ref. 12), and Rajchl (ref. 13). An electron density for this meteor was inferred from electron line densities of meteors with similar brightness and velocity. The lower electron density at the higher altitude of this meteor compared with the electron densities at the altitudes of the brighter meteors of references 8 to 10 probably explains the H- and K-line behavior. Merely

note that this behavior is not grossly anomalous in this spectrum. The strongest feature in the spectrum is the unresolved multiplet 3 of MgI and multiplet 20 of FeI centered near 3830 Å. The strength and number of lines in the near-ultraviolet are explained by the transmission properties of the fused silica of the refractive elements in the lens system, the enhanced blue sensitivity of the Kodak 2485 emulsion, and the blue blaze of the grating. Previous-generation meteor spectrographs generally used soda- and lead-glass transmission elements.

ANALYSIS

Wavelength Identifications

The features in the spectrum are listed in table I. Sixty-three definitive features in the spectral range from 3000 Å to 6800 Å were measured on the microdensitometer tracing. Thus, the meteor spectrum is in class "a" (more than 49 lines) of Millman's (ref. 14) spectral classification scheme. Identifications of the features were checked with high-dispersion spectra (refs. 10 and 15) and with oscillator strengths (ref. 16). If a tentative identification was not consistent with these criteria, the feature was left unidentified. Three features were unidentified. The wavelengths λ_m in table I are those from the densitometer tracing; the wavelengths λ_{tab} are those identified, and are from Corliss and Bozman (ref. 16) and Moore (ref. 17). The multiplets and elements are from Moore (ref. 17), the products of the statistical weights and the Einstein probability coefficients, gA , are primarily from Corliss and Bozman (ref. 16), and the energy levels E_1 and E_2 are from Moore (ref. 17). Nine elements - iron, calcium, nickel, magnesium, nitrogen, oxygen, sodium, silicon, and hydrogen - were identified in the spectrum.

Photometry

The photometry is essentially that developed by Harvey (ref. 18), except for extension to a wider wavelength interval. The writing speed of the meteor image across the film was computed from the radiant position determined from the plate, the spectrograph elevation angle and focal length, and the meteor velocity at maximum light for an assumed height of 100 km. This height is based upon termination of the auroral green line of OI (ref. 19) and the height of maximum brightness of similar meteors (ref. 20). The estimated height uncertainty is several kilometers and introduces an uncertainty of the order of 10 percent in the absolute irradiance. This is the same order as other errors in the photometry.

A densitometer tracing of the meteor spectrum at the point of maximum brightness is shown in figure 2. The spectral irradiances of the multiplets of interest were obtained by reading the maximum intensity from a grid of contours of constant irradiance and multiplying by a half-width based on the plate resolution and the multiplet width. Thus, the irradiance values obtained are analogous to the equivalent widths used in studies of stellar atmospheres. The spectral irradiance was corrected for the emulsion sensitivity, atmospheric transmission, spectrograph transmission, and grating blaze efficiency.

Meteor Magnitude and Meteoroid Mass

The absolute magnitude and the statistical mass of this meteor were obtained by comparing the spectral irradiance of the meteor in the spectral region from 3200 Å to 4800 Å with the spectral irradiance of a -0.5 magnitude iron artificial meteor in this spectral region (ref. 21). An absolute photographic magnitude of -1.5 (or approximately zero visual magnitude) was obtained for this meteor.

Artificial meteor experiments have determined the luminous efficiency of iron at low meteoric velocities to within ± 10 percent (ref. 1). This luminous efficiency may be used in conjunction with two results from the Smithsonian Astrophysical Observatory (SAO) - one relating the luminous efficiency of iron to that of natural meteors (ref. 22), and the other determining the dependence of the luminous efficiency upon velocity (ref. 23) - to compute the mass of the meteoroid. The computations yield a value of 9 mg for the mass of the meteoroid.

Effective Radiation Temperature

Spectral irradiance is proportional to line intensity; thus, photometrically corrected spectral irradiance line ratios and absolute atomic emission line ratios from the corresponding energy levels are equal. The line intensity ratio (irradiance ratio) for an optically thin gas in local thermodynamic equilibrium is given by

$$\frac{I_i}{I_j} = \frac{h \nu_i N_i A_i}{h \nu_j N_j A_j} = \frac{h \nu_i g_i A_i}{h \nu_j g_j A_j} e^{-(E_i - E_j)/kT} \quad (1)$$

where N_i is the number of particles in the i th atomic state with energy E_i above the ground state, h is Planck's constant, ν_i is the frequency of observed radiation from the i th state, g_i is the statistical weight of the i th state, A_i is the Einstein probability coefficient of the i th state, k is the Boltzmann constant, and T is the temperature. Even if the meteor plasma is not in local thermodynamic equilibrium, equation (1) can be used to compute a parameter analogous to the temperature for each choice of a pair of upper energy levels obtained from the observed irradiance ratios. This parameter can be used to study the gas. It is designated herein the "meteor temperature parameter T_{ij}^* ", and an average of T_{ij}^* is the "effective meteor radiation temperature."

Multiplet irradiance ratios were obtained from figure 2 and were used to calculate the meteor temperature parameters T_{ij}^* . Many of the spectral identifications were blends of lines; therefore, multiplets and not individual lines were used for the T_{ij}^* determinations. Those multiplets which appeared to be reasonably uncontaminated by other multiplets for intensity determinations are listed in table II. The values for T_{ij}^* calculated from the multiplets of table II are listed in table III. Since the magnesium lines in the meteor

spectrum were contaminated by iron lines, only iron multiplets were used to compute T_{ij}^* . An effective radiation temperature of 5730 ± 670 K was obtained for this meteor.

The general agreement in T_{ij}^* from different multiplets of similar levels, as shown in table III, indicates that assigning a temperature for energy levels in that range is justified. The sensitivity of the multiplet irradiance ratios can easily be checked via the Boltzmann formula. For an uncertainty in temperature of ± 670 K (for a temperature of 5730 K and for the energy levels of multiplets 5 and 41 of FeI), a corresponding mean uncertainty of 19 percent results in the irradiance ratio based on the Boltzmann distribution.

Element Ratios

The effective radiation temperature can be used to compute relative abundances of the dominant radiating elements with the caution that departures from local thermodynamic equilibrium in the plasma may introduce errors in the results. Other uncertainties are introduced by ionization, self-absorption, dissociation, and blending of lines. The Boltzmann equation can be written in the more general form,

$$\frac{N_{a,i}}{N_a} = \frac{g_i}{B_a(T)} e^{-E_i/kT} \quad (2)$$

where N_a is the total number of atoms of the element a in a given stage of ionization and $N_{a,i}$ is the number of atoms in atomic state i for that stage of ionization; $B_a(T)$ is the partition function of element a . The corresponding equation for line intensities is

$$I_{a,i} = h\nu_i g_{a,i} A_{a,i} \frac{N_a}{B_a(T)} e^{-E_i/kT} \quad (3)$$

for an element a . From this the number ratio of elements a and b can be obtained:

$$\frac{N_a}{N_b} = \frac{I_{a,i}}{I_{b,j}} \frac{B_a(T)}{B_b(T)} \frac{g_{b,j} A_{b,j} \nu_{b,j}}{g_{a,i} A_{a,i} \nu_{a,i}} e^{-(E_j - E_i)/kT} \quad (4)$$

By using partition functions from Corliss (ref. 24) and T_{ij}^* for T , the following weight ratios were calculated:

$$\text{CaI:FeI} = 0.052:1$$

$$\text{MgI:FeI} = 1.35:1$$

$$\text{NaI:FeI} = 0.012:1$$

Because of the many uncertainties inherent in these calculations, these ratios are assumed to have only an order of magnitude of accuracy, and the results from this part of the analysis can be summarized as follows:

$$\text{CaI:FeI} = 0.05:1$$

$$\text{MgI:FeI} = 1:1$$

$$\text{NaI:FeI} = 0.01:1$$

METEOR PLASMA PARTICLE SPEEDS

Derivation of Particle Speed Distributions

Consider a "typical" faint optical meteoroid with mass of approximately 0.01 g and density of approximately 1 g/cm^3 . If this meteoroid is assumed to be spherical, it would have estimated linear dimensions of approximately 2.7 mm. At a typical meteor height of 90 km, the molecular mean free path is approximately 2.5 cm. Thus, the free molecular flow condition is easily satisfied.

As the meteoroid passes through the rarefied gas at this height, the air molecules impact the meteoroid, and as a result, either atoms or small pieces of meteoroid leave the parent meteoroid with virtually undiminished velocity relative to the atmosphere. This process continues and results in a cloud of meteoric atoms immediately detached from the meteoroid and moving in the air-stream with nearly the initial speed of the meteoroid. However, the masses of the individual atoms are nearly equal to the masses of the atmospheric molecules. Thus, collisions are efficient in decelerating and exciting meteoric atoms because of favorable momentum transfer. One may visualize a cloud of meteoric atoms initially moving at nearly the initial meteoroid speed. Then the atoms give up their energy to the atmosphere in a series of collisions with air molecules. For meteoroids in free molecular flow, the meteoric process just described is similar to the model for faint meteors formulated by Öpik (ref. 25).

Let $N_m(V)$ be the number distribution of particles of speed V in the meteor plasma, ℓ be the atmospheric mean free path length, and $N_0 = \frac{1}{m} \frac{dM}{ds}$ be the number of meteoric particles entering the meteor plasma per unit distance along the meteor trail (M is the mass of the meteoroid). The number of meteoric particles in the speed interval from V_0 to $V_0 + \Delta V$ is $N_m(V) \Delta V$.

The speed distribution can be obtained either by looking at all particles at one time or by following in time a set of particles as they decrease in speed by undergoing collisions; that is,

$$N_m(V) \Delta V = N_m(t) \Delta t \quad (5)$$

where $\Delta V = V_0 - V_1$, $\Delta t = t_0 - t_1$, V_0 is the average particle speed in the plasma at time t_0 after being sputtered by the meteoroid, and V_1 is the average particle speed in the meteor plasma at time t_1 . The number of meteoric particles does not change with time; therefore, $N_m(t) = N_0$ and

$$N_m(V) \Delta V = N_0(t_0 - t_1)$$

Since $t_0 = \ell/V_0$ and $t_1 = \ell/V_1$ for each collision,

$$\begin{aligned} N_m(V) \Delta V &= N_0 \left(\frac{\ell}{V_0} - \frac{\ell}{V_1} \right) \\ &= N_0 \ell \frac{-\Delta V}{V_0 V_1} \end{aligned}$$

which in the limit becomes

$$N_m(V) dV = -N_0 \ell \frac{dV}{V^2} \quad (6)$$

In contrast, for a gas in local thermodynamic equilibrium, the speed distribution of particles of speed V is given by the Boltzmann distribution:

$$N_B(V) dV = CT^{-2/3} V^2 e^{-C'V^2/T} dV \quad (7)$$

where C and C' are constants and T is the temperature.

The average speed for the cascading system is

$$\bar{V} = \frac{\int_{V_1}^{V_0} V N(V) dV}{\int_{V_1}^{V_0} N(V) dV} \quad (8)$$

Substituting equation (6) and integrating results in

$$\bar{v}_m = \frac{v_1 v_0 \ln (v_0/v_1)}{v_0 - v_1} \quad (9)$$

where v_0 is the initial meteoroid speed relative to the atmosphere and v_1 is the lowest characteristic speed of atoms in the meteor plasma for which excitation occurs. For the present example, the extreme case is assumed; that is, $v_0 = 72$ km/sec (the upper limit for meteoroids) and $v_1 = 0.9$ km/sec (the average speed of iron atoms at 1800 K, the melting temperature of iron). Then, from equation (9),

$$\bar{v}_m = 4.0 \text{ km/sec}$$

Similarly, the energy-averaged speed (root-mean-square speed) for the cascade system can be calculated to be

$$(v_{rms})_m = \sqrt{v_1 v_0} = 8 \text{ km/sec}$$

These speeds which may characterize high-velocity meteor plasmas can be compared with those for a Boltzmann distribution by using equation (7) and equation (8) to obtain

$$\bar{v}_B = \frac{1}{N} \int_0^{\infty} v N_B(v) dv = \sqrt{\frac{8kT}{\pi m}}$$

Using 5700 K, the effective radiation temperature of the high-velocity meteor, for T and the mass of an iron atom for m gives

$$\bar{v}_B = 1.5 \text{ km/sec}$$

The relative collision speed v_r , which is the relevant speed for excitations, for two unlike particles with average speeds \bar{v}_a and \bar{v}_b in a Boltzmann gas (ref. 26) is

$$v_r = (\bar{v}_a^2 + \bar{v}_b^2)^{1/2}$$

For iron atoms and air molecules at 5700 K,

$$V_r = \sqrt{3} \bar{V}_{Fe} = 2.8 \text{ km/sec}$$

Thus, the average or characteristic collision speeds of particles of a meteor plasma derived from an inverse square velocity distribution of meteoric atoms (\bar{V}_m) generally agree with the average or characteristic speeds obtained from the observed spectra by assuming a Boltzmann speed distribution (V_r). These meteor plasma characteristic particle speeds are more than an order of magnitude lower than the initial meteoroid speed.

Collision Speed and Radiation

From table I in conjunction with figure 2, it can be seen that, in general, the low energy levels (3.0 to 4.5 eV) of the atoms are heavily populated and intermediate and higher levels (greater than 4.5 eV) are sparsely populated. For example, multiplet 5 of FeI in the wavelength range from 3720 Å to 3750 Å is very strong, but intrinsically strong lines at 3686 Å, 3694 Å, and 3701 Å of multiplets 386 and 394 are not detected in the spectrum. The upper energy level of multiplet 5 is 3.3 eV. The upper energy level of multiplets 386 and 394 is 6.3 eV. Most plasmas tend to emit most of their radiation at energies almost an order of magnitude greater than the characteristic speeds of the particles. This generally observed phenomenon is predicted for blackbody radiation by Wein's displacement law ($\lambda_{\max}T = \text{Constant}$) and the definitions of most probable, average, or rms speeds ($V \approx \sqrt{2kT/m}$). The cascade model gives a rms speed for the cascade of atoms from meteoroid speed, 72 km/sec, to 0.9 km/sec of approximately 8 km/sec. The cascade velocity distribution could explain the general lack of extremely high (greater than 10 eV) excitation and ionization of meteoric atoms (i.e., excitation and ionization comparable with the meteoroid velocity). However, even the collision-driven speed distribution of the cascading system results in a higher average relative particle speed, 4.0 km/sec, than that inferred from the observed spectra, 2.8 km/sec. Thus, the actual meteor spectra may indicate that the higher energy levels of the atoms are less populated than may be predicted by a simple velocity cascading system. This may result because some of the radiation may not occur during the main downward cascade in velocity of the meteoric atoms but rather during the relaxation of the heated atmospheric-meteoric plasma after passage of the meteoroid. Thus, the radiation may be even more nearly in thermodynamic equilibrium than indicated by cascade excitation. This is consistent with the strength and time behavior of the ground-state transitions observed in chopped meteor spectra and meteor flares (ref. 27).

CONCLUDING REMARKS

Analysis of the spectrogram of a high-velocity optical meteor indicates that although the initial meteoroid entry velocity was 60 km/sec or higher (allowing maximum excitation energies over 500 eV), most of the radiation from the meteor is due to transitions from less energetic states (3.0 to 4.5 eV).

This implies that the colliding particles responsible for the excitations have a speed distribution characterized by average speeds considerably less than the initial meteoroid velocity. This in turn is an indication that the meteoric plasma may, for some purposes, be approaching conditions of local thermodynamic equilibrium and that the Boltzmann relationships may be profitably used to gain insight into the conditions of the meteoric plasma and the elemental abundances of the meteoroid.

A comparison of the particle speed distribution predicted by a simple velocity cascade model for meteor atoms deceleration with the Boltzmann speed distribution provides an indication of the degree of local thermodynamic equilibrium for the meteoric plasma. The average relative collision speed predicted by the model is 4.0 km/sec which compares with 2.8 km/sec for average relative collision speed derived from the observed spectrum with a Boltzmann equation.

Using the Boltzmann relationships, an "effective radiation temperature" of 5730 ± 670 K was calculated for the high-velocity meteor on the basis of ratios of FeI multiplet transitions identified in the spectrum.

The Boltzmann relationship was also used to calculate relative weight ratios of neutral elements identified in the spectrum. To an estimated order of magnitude accuracy, the results of the calculations are

CaI:FeI = 0.05:1

MgI:FeI = 1:1

NaI:FeI = 0.01:1

Langley Research Center
National Aeronautics and Space Administration
Hampton, VA 23666
May 31, 1977

REFERENCES

1. Ayers, W. G.; McCrosky, R. E.; and Shao, C.-Y.: Photographic Observations of 10 Artificial Meteors. Spec. Rep. No. 317, Smithsonian Inst. Astrophys. Obs., June 5, 1970.
2. Harvey, Gale A.: The NASA LRC Faint Meteor Spectra Patrol. NASA TN D-6298, 1971.
3. Ceplecha, Z.: Study of a Bright Meteor Flare by Means of Emission Curve of Growth. Bull. Astron. Inst. Czechoslovakia, vol. 15, no. 3, 1964, pp. 102-112.
4. Ceplecha, Z.: Spectroscopic Analysis of Iron Meteoroid Radiation. Bull. Astron. Inst. Czechoslovakia, vol. 18, no. 5, 1967, pp.303-310.
5. Russell, John A.: Molecular Nitrogen in the Spectra of Two Perseid Meteors. Publ. Astron. Soc. Pacific, vol. 72, no. 427, 1960, pp. 291-295.
6. Millman, P. M.; Cook, A. F.; and Hemenway, C. L.: Spectroscopy of Perseid Meteors With an Image Orthicon. Canadian J. Phys., vol. 49, no. 10, May 15, 1971, pp. 1365-1373.
7. Russell, John A.: The Spectra of Faint Perseids. Meteoritics, vol. 2, no. 2, Feb. 1964, pp. 117-125.
8. Etheridge, Dale A.; and Russell, John A.: The Spectrum of a Meteor From the 1966 Leonid Shower. Publ. Astron. Soc. Pacific, vol. 80, no. 476, Oct. 1968, pp. 550-554.
9. Hirose, H.; Nagasawa, K.; and Tomita, K.: Spectral Studies of Meteors at the Tokyo Astronomical Observatory. Physics and Dynamics of Meteors, Luber Kresák and Peter M. Millman, eds., Springer-Verlag New York, Inc., 1968, pp. 105-118.
10. Halliday, Ian: A Study of Spectral Line Identifications in Perseid Meteor Spectra. Publ. Dominion Obs. Ottawa, vol. XXV, no. 1, 1961, pp. 3-16.
11. Hoffman, Herbert S.: Ionic Spectra of Meteors. Astrophys. J., vol. 163, no. 2, pt. 1, Jan. 15, 1971, pp. 393-403.
12. Harvey, Gale A.: The Calcium H- and K-Line Anomaly in Meteor Spectra. Astrophys. J., vol. 165, no. 3, pt. 1, May 1, 1971, pp. 669-671.
13. Rajchl, J.: A Short Note on Meteor Spectra With Low Dispersion. Smithsonian Contrib. Astrophys., vol. 7, 1963, pp. 155-156.
14. Millman, Peter M.: A General Survey of Meteor Spectra. Smithsonian Contrib. Astrophys., vol. 7, 1963, pp. 119-127.

15. Halliday, Ian: A Study of Ultraviolet Meteor Spectra. Publ. Dominion Obs. Ottawa, vol. XXV, no. 12, 1969, pp. 315-322.
16. Corliss, Charles H.; and Bozman, William R.: Experimental Transition Probabilities for Spectral Lines of Seventy Elements. NBS Monogr. 53, U.S. Dep. Commer., July 20, 1962.
17. Moore, Charlotte E.: A Multiplet Table of Astrophysical Interest - Revised Edition. NSB Tech. Note 36 (PB I51395), U.S. Dep. Commer., Nov. 1959.
18. Harvey, Gale A.: A Method of Slitless Absolute Spectral Photometry. NASA TN D-3765, 1967.
19. Halliday, Ian: Auroral Green Line in Meteor Wakes. Astrophys. J., vol. 131, no. 1, Jan. 1960, pp. 25-33.
20. Jacchia, Luigi G.; Verniani, Franco; and Briggs, Robert E.: An Analysis of the Atmospheric Trajectories of 413 Precisely Reduced Photographic Meteors. Spec. Rep. No. 175, Smithsonian Inst. Astrophys. Obs., Apr. 23, 1965.
21. Harvey, Gale A.: Photometry of Spectrograms of Three Artificial Meteors. NASA TN D-3930, 1967.
22. Cook, A. F.; Jacchia, L. G.; and McCrosky, R. E.: Luminous Efficiency of Iron and Stone Asteroidal Meteors. Smithsonian Contrib. Astrophys., vol. 7, 1963, pp. 209-220.
23. Verniani, Franco: On the Luminous Efficiency of Meteors. Spec. Rep. No. 145, Smithsonian Inst. Astrophys. Obs., Feb. 17, 1964.
24. Corliss, Charles H.: Ionization in the Plasma of a Copper Arc. J. Res. Natl. Bur. Stand., Sect. A, vol. 66A, no. 2, Mar.-Apr. 1962, pp. 169-175.
25. Öpik, Ernst: Atomic Collisions and Radiation of Meteors. Reprint 100, Harvard Univ. (From Acta et Commentationes Universitatis Tartuensis (Dorpatensis) A XXVI.2, 1933.)
26. Present, R. D.: Kinetic Theory of Gases. McGraw-Hill Book Co., Inc., 1958.
27. Halliday, Ian: Diffusion Effects Observed in the Wake Spectrum of a Geminid Meteor. Smithsonian Contrib. Astrophys., 1963, pp. 161-169.

TABLE I.- WAVELENGTH TABLE

λ_m , Å	λ_{tab} , Å	Multiplet and element	gA , 10^8 /sec	E_1 , eV	E_2 , eV
3020	3020.5	9 FeI	1.4	0.09	4.17
	3020.6	9 FeI	5.5	0	4.09
	3021.1	9 FeI	3.5	.05	4.14
3110	3099.9	28 FeI	8.6	1.01	4.99
	3100.3	28 FeI	3.9	.99	4.97
	3100.7	28 FeI	3.6	.95	4.95
3195	3192.9	6 FeII	.14	1.66	5.53
	3193.2	7 FeI		0	3.86
	3193.8	6 FeII		1.72	5.58
	3196.1	7 FeII		1.66	5.52
3225	3227.8	6 FeII	79	1.66	5.49
3280	3277.3	1 FeII		.98	4.75
3310	3306.0	91 FeI	38	2.19	5.92
	3306.4	91 FeI	40	2.21	5.95
3370	3369.6	6 NiI	2.1	0	3.66
3440	3440.6	6 FeI	2.8	0	3.59
	3441.0	6 FeI	.64	.05	3.64
	3443.9	6 FeI	.34	.09	3.67
3480	3475.4	6 FeI	.64	.09	3.64
	3476.7	6 FeI	.28	.12	3.67
	3490.6	6 FeI	.58	.05	3.59
3533	3533.2	326 FeI	23	2.87	6.36
	3536.6	326 FeI	56	2.86	6.35
	3541.1	326 FeI	65	2.84	6.32
	3542.1	326 FeI	61	2.85	6.34
3570	3555.0	326 FeI	73	2.82	6.29
	3558.5	24 FeI	3.5	.99	4.45
	3565.4	24 FeI	7.8	.95	4.42
	3570.1	24 FeI	18	.91	4.37
	3581.2	23 FeI	23	.86	4.30
3610	3608.9	23 FeI	10	1.01	4.43
	3618.8	23 FeI	9.5	.99	4.40

TABLE I.- Continued

λ_m , Å	λ_{tab} , Å	Multiplet and element	gA , $10^8/\text{sec}$	E_1 , eV	E_2 , eV
3680	3683.1	5 FeI	0.055	0.05	3.40
3738	3719.9	5 FeI	2.5	0	3.32
	3734.9	21 FeI	20	.86	4.16
	3737.1	5 FeI	1.5	.05	3.35
	3745.6	5 FeI	1.2	.09	3.38
	3748.3	5 FeI	.71	.11	3.40
	3749.5	21 FeI	13	.91	4.20
	3825	3820.4	20 FeI	12	.86
3829.4		3 MgI	11	2.70	5.92
3832.3		3 MgI	23	2.70	5.92
3838.3		3 MgI	39	2.70	5.92
3824.4		4 FeI	.28	0	3.23
3825.9		20 FeI	8.9	.91	4.14
3834.2		20 FeI	3.9	.95	4.17
3840.4		20 FeI	2.6	.99	4.20
3855	3856.4	4 FeI	.31	.05	3.25
	3859.9	4 FeI	1.4	0	3.20
3886	3886.3	4 FeI	.63	.09	3.27
3930	3920.3	4 FeI	.14	.12	3.27
	3922.9	4 FeI	.18	.05	3.20
	3927.9	4 FeI	.26	.11	3.25
	3930.3	4 FeI	.27	.09	3.23
	3933.7	1 CaII	.91	0	3.14
	3947.3	3 OI	.05	9.11	12.23
3962	3956.7	278 FeI	9.1	2.68	5.80
	3966.1	45 FeI	.43	1.60	4.71
	3969.3	43 FeI	4.4	1.48	4.59
	3968.5	1 CaII	.45	0	3.11
4040	4045.8	43 FeI	22	1.48	4.53
4064	4063.6	43 FeI	9.9	1.55	4.59
	4071.7	43 FeI	9.1	1.60	4.63
4110	4110.0	10 NI	.24	10.64	13.65

TABLE I.- Continued

λ_m , Å	λ_{tab} , Å	Multiplet and element	gA , $10^8/\text{sec}$	E_1 , eV	E_2 , eV
4145	4143.9	43 FeI	2.9	1.55	4.53
	4151.5	6 NI	.05	10.29	13.26
4225	4216.2	3 FeI	.0031	0	2.93
	4226.7	2 CaI	1.0	0	2.92
	4223.0	5 NI	.30	10.29	13.21
	4224.7	5 NI	.12	10.29	13.21
	4230.4	5 NI	.13	10.29	13.21
	4233.6	152 FeI	5.9	2.47	5.39
	4235.9	152 FeI	7.9	2.41	5.33
4257	4260.5	152 FeI	15	2.39	5.29
	4271.8	42 FeI	5.2	1.48	4.37
4308	4307.9	42 FeI	5.9	1.55	4.42
	4325.8	42 FeI	6.1	1.60	4.45
4375	4368.3	5 OI	.06	9.48	12.31
	4375.9	2 FeI	.0094	0	2.82
	4383.6	41 FeI	7.7	1.48	4.29
4420	4427.3	2 FeI	.0099	.05	2.84
4478	4481.2	4 MgII	31.5	8.83	11.58
4526	4520.2	37 FeII		2.79	2.52
	4522.6	38 FeII		2.83	5.56
4554	4549.5	38 FeII		2.82	5.53
	4555.9	37 FeII		2.82	5.52
4572	4571.1	1 MgI	.000013	0	2.70
4610		Unidentified			
4656	4654.2	18 OI		10.69	13.35
	4654.6	18 OI		10.69	13.35
	4655.4	18 OI		10.69	13.35
4690		Unidentified			
4768	4772.5	16 OI		10.69	13.28
	4772.9	16 OI		10.69	13.28
	4773.8	16 OI		10.69	13.28

TABLE I.- Continued

λ_m , Å	λ_{tab} , Å	Multiplet and element	gA , $10^8/\text{sec}$	E_1 , eV	E_2 , eV
4880	4859.7	318 FeI	1.3	2.86	5.40
	4871.3	318 FeI	3.7	2.87	5.39
	4872.2	318 FeI	2.2	2.87	5.40
	4878.2	318 FeI	.77	2.87	5.40
4955	4957.3	318 FeI	2.2	2.84	5.33
	4957.6	318 FeI	6.4	2.80	5.29
5180	5166.3	1 FeI		0	2.39
	5167.34	2 MgI	1.2	2.70	5.09
	5167.4	37 FeI	.26	1.48	3.87
	5171.6	36 FeI	.12	1.48	3.86
	5172.7	2 MgI	3.5	2.70	5.09
	5183.6	2 MgI	6.4	2.70	5.09
5220		Unidentified			
5280	5269.5	15 FeI	.098	.86	3.20
	5270.4	37 FeI	.20	1.60	3.94
5336	5329.0	12 OI	.49	10.69	13.01
	5329.6	12 OI		10.69	13.01
	5330.7	12 OI		10.69	13.01
5376	5371.5	15 FeI	.062	.95	3.25
5406	5405.8	15 FeI	.038	.99	3.27
5440	5434.5	15 FeI	.028	1.01	3.28
	5435.2	11 OI	.15	10.69	12.96
	5435.8	11 OI	.15	10.69	12.96
	5436.8	11 OI	.15	10.69	12.96
	5446.9	15 FeI	.031	.99	3.25
5525	5528.4	9 MgI	1.6	4.33	6.56
5577	5577.4	3F OI		1.96	4.17
5710	5708.4	10 SiI		4.93	7.09
5747	5755.2	12,8 N ₂ 1+		7.52	9.67
5780	5772.3	17 SiI		5.06	7.20

TABLE I.- Concluded

λ_m , Å	λ_{tab} , Å	Multiplet and element	gA , $10^8/\text{sec}$	E_1 , eV	E_2 , eV
5889	5889.9	1 NaI	1.8	0	2.10
	5895.9	1 NaI	.90	0	2.09
5953	5957.6	4 SiIII	.356	10.02	12.09
5990	5979.0	4 SiIII	.527	10.03	12.09
6153	6156.0	10 OI	1.7	10.69	12.70
	6156.8	10 OI		10.69	12.70
	6158.2	10 OI		10.69	12.70
6240	6247.6	74 FeII		3.87	5.85
6300	6322.9	10,7 N ₂ 1+		7.37	9.32
6350	6347.1	2 SiIII	2.8	8.09	10.03
6371	6371.4	2 SiIII	1.4	8.09	10.02
6460	6456.0	9 OI	.35	10.69	12.61
6490	6493.8	18 CaI	1.4	2.51	4.41
	6495.0	168 FeI	.20	2.39	4.29
6580	6572.8	1 CaI	.00021	0	1.88
	6562.8	1 HI	7.94	10.15	12.04
6660	6656	6,3 N ₂ 1+		6.72	8.58
6740	6726	2 OI		9.11	10.94

TABLE II.- PRINCIPAL MULTIPLETS IN METEOR SPECTRUM

Element	Multiplet	$\Sigma gA,$ $10^8/\text{sec}$	$E_2,$ eV
FeI	5	7.0	3.35
FeI	6	3.8	3.64
FeI	23	19.5	4.42
FeI	23-24	52.3	4.40
FeI	41	17.1	4.30
FeI	42	12.0	4.44
FeI	43	41.0	4.58
MgI	3	73	5.92
MgI	2	11.1	5.09
CaI	2	1.0	2.92
NaI	1	2.7	2.10

TABLE III.- T_{1j}^* CALCULATED FROM EQUATION (1) USING
MULTIPLETS IN TABLE II

Element	Multiplets	Meteor temperature parameter, T_{1j}^* , K
FeI	5,23-24	5190
FeI	5,41	5310
FeI	5,43	6110
FeI	6,23-24	4780
FeI	6,42	6350
FeI	6,23	6620
Average		5727
Standard error		670

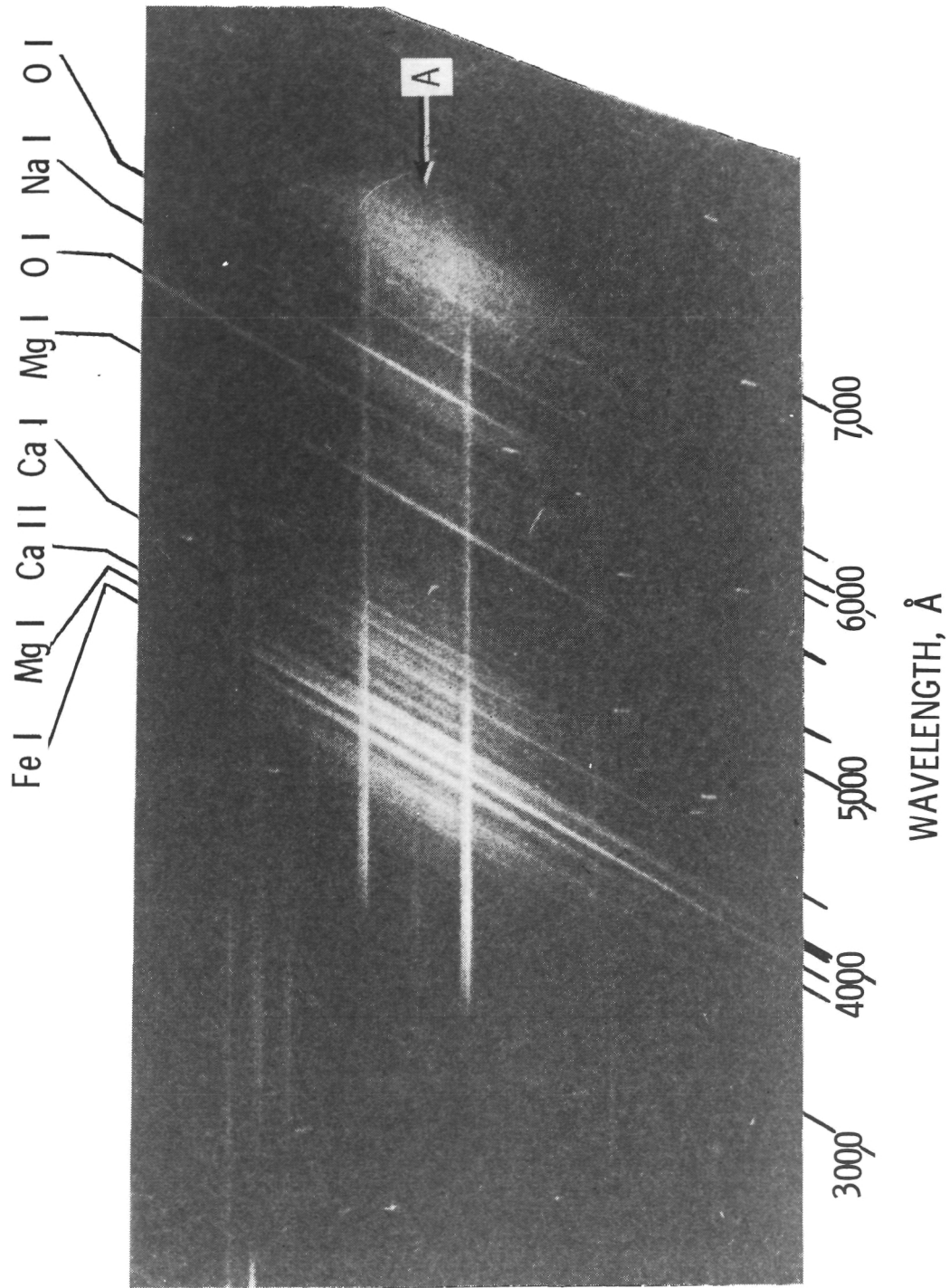


Figure 1.- Spectrum of high-velocity meteor photographed on November 21, 1968, over southern New Mexico.

L-77-210

Contour lines represent constant irradiance in 10^{-8} ergs-cm²-Å-sec at a distance of 100 km from the source

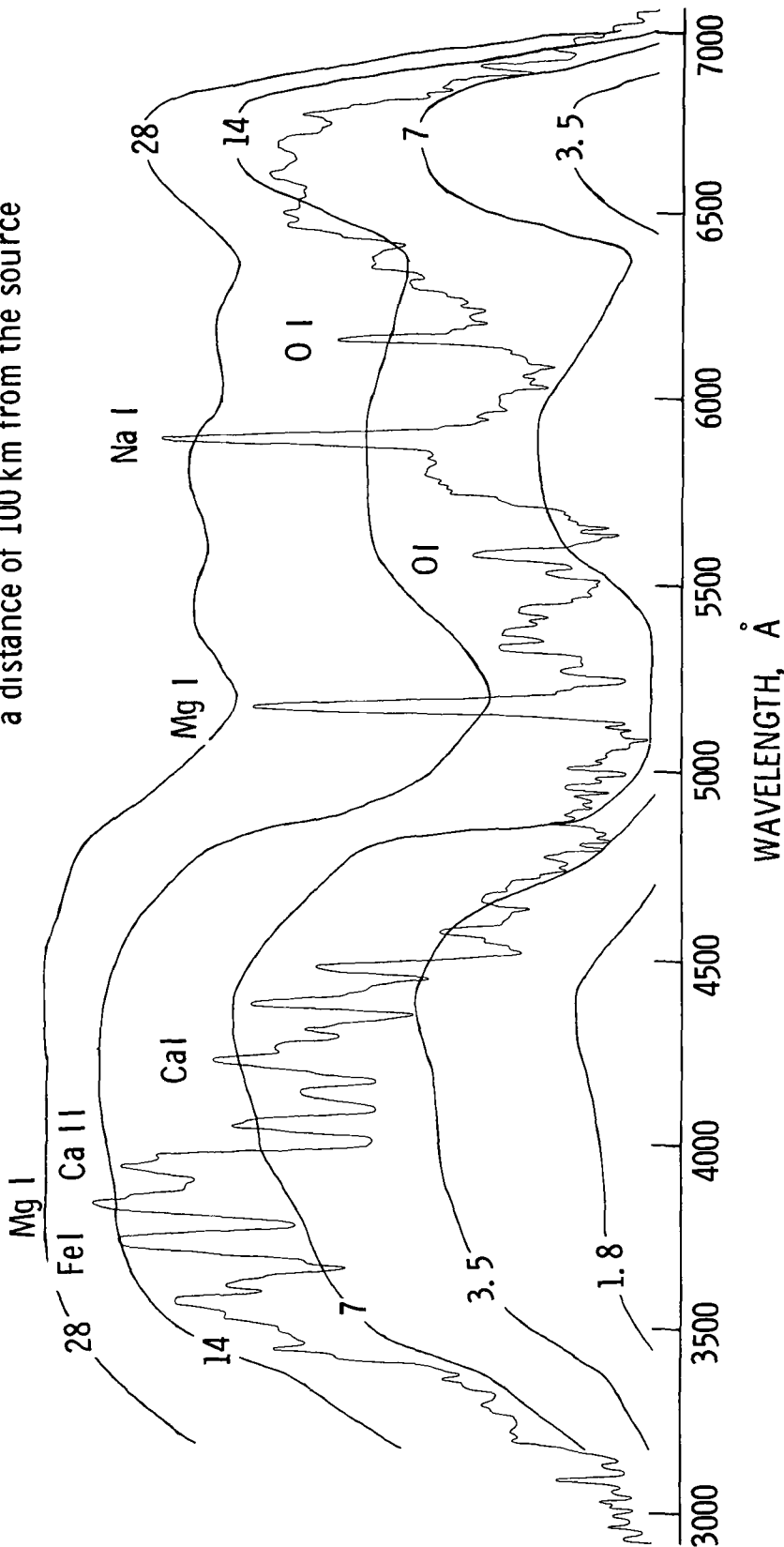


Figure 2.- Densitometer tracing of meteor spectrum from position A (fig. 1) along trail.



POSTMASTER

If Undeliverable (Section 158
Postal Manual) Do Not Return

"The aeronautical and space activities of the United States shall be conducted so as to contribute . . . to the expansion of human knowledge of phenomena in the atmosphere and space. The Administration shall provide for the widest practicable and appropriate dissemination of information concerning its activities and the results thereof."

—NATIONAL AERONAUTICS AND SPACE ACT OF 1958

NASA SCIENTIFIC AND TECHNICAL PUBLICATIONS

TECHNICAL REPORTS Scientific and technical information considered important, complete, and a lasting contribution to existing knowledge

TECHNICAL NOTES Information less broad in scope but nevertheless of importance as a contribution to existing knowledge

TECHNICAL MEMORANDUMS Information receiving limited distribution because of preliminary data, security classification, or other reasons. Also includes conference proceedings with either limited or unlimited distribution.

CONTRACTOR REPORTS Scientific and technical information generated under a NASA contract or grant and considered an important contribution to existing knowledge

TECHNICAL TRANSLATIONS Information published in a foreign language considered to merit NASA distribution in English

SPECIAL PUBLICATIONS Information derived from or of value to NASA activities. Publications include final reports of major projects, monographs, data compilations, handbooks, sourcebooks, and special bibliographies.

TECHNOLOGY UTILIZATION PUBLICATIONS Information on technology used by NASA that may be of particular interest in commercial and other non-aerospace applications. Publications include Tech Briefs, Technology Utilization Reports and Technology Surveys

Details on the availability of these publications may be obtained from:

SCIENTIFIC AND TECHNICAL INFORMATION OFFICE

NATIONAL AERONAUTICS AND SPACE ADMINISTRATION

Washington, D.C. 20546